HHS Public Access

Author manuscript

Biol Psychiatry. Author manuscript; available in PMC 2018 February 15.

Published in final edited form as:

Biol Psychiatry. 2017 February 15; 81(4): 306–315. doi:10.1016/j.biopsych.2016.08.017.

DCC confers susceptibility to depression-like behaviors in humans and mice and is regulated by miR-218

Angélica Torres-Berrío[1,2,*], **Juan Pablo Lopez**[3,4,*], **Rosemary C. Bagot**[5], **Dominique Nouel**[2], **Gregory Dal-Bo**[2,6], **Santiago Cuesta**[2,7], **Lei Zhu**[2], **Colleen Manitt**[2], **Conrad Eng**[2], **Helen Cooper**[8], **Florian Storch**[2,7], **Gustavo Turecki**[2,4,7], **Eric J. Nestler**[9], and **Cecilia Flores**[2,7,†]

[1]Integrated Program in Neuroscience, McGill University, Montréal, Québec, Canada

[2]Douglas Mental Health University Institute, Montréal, Québec, Canada

[3]Department of Human Genetics, Montréal, Québec, Canada

[4]McGill Group for Suicide Studies, Montréal, Québec, Canada

[5]Department of Psychology, McGill University, Montréal, Québec, Canada

[6]Département de Toxicologie et risques chimiques, IRBA, Brétigny sur Orge, France

[7]Department of Psychiatry, McGill University, Montréal, Québec, Canada

[8]The University of Queensland, Queensland Brain Institute, Brisbane, QLD, Australia

[9]Fishberg Department of Neuroscience and Friedman Brain Institute, Icahn School of Medicine at Mount Sinai, New York, NY USA

Abstract

BACKGROUD—Variations in the expression of the Netrin-1 guidance cue receptor *DCC* (Deleted in colorectal cancer) appear to confer resilience or susceptibility to psychopathologies involving prefrontal cortex (PFC) dysfunction.

[†]To whom correspondence may be addressed: Cecilia Flores, Douglas Mental Health University Institute, Department of Psychiatry, McGill University, 6875 Boulevard LaSalle, Montreal, Quebec, H4H 1R3, Tel: (+1)514 761 6131; Ext: 2814, cecilia.flores@mcgill.ca.
[*]These authors contributed equally to this work.

DISCLOSURES

All authors report no biomedical financial interests or potential conflicts of interest.

CONTRIBUTIONS

A.T.B., J.P.L., and C.F. designed the project. A.T.B, J.P.L. performed expression experiments with postmortem human brain samples and mouse brain tissue. A.T.B. performed stereotaxic surgeries, viral infections, and behavioral and in vitro experiments. D.N, and G.D.B. performed all the neuroanatomical experiment. R.C.B. performed behavioral and expression experiments in mouse tissue. S.C. and L.Z. performed cell cultures. C.M. and C.E. conducted immunofluorescent experiments in mouse tissue. H. C. and F.S. provided scientific advice and reagents. E.J. N. and G.T., provided reagents and technical training necessary to perform the research. A.T.B and C.F. wrote the manuscript C.F. conceived and designed the study and supervised the project. All authors discussed the results and commented and edited the manuscript.

METHODS—Using postmortem brain tissue, mouse models of defeat stress, and in vitro analysis, we assessed microRNA (miRNA) regulation of *DCC* and whether changes in *DCC* levels in the PFC lead to vulnerability to depression-like behaviors.

RESULTS—We identify miR-218 as a posttranscriptional repressor of *DCC,* and detect co-expression of *DCC* and miR-218 in pyramidal neurons of human and mouse PFC. We find that exaggerated expression of *DCC* and reduced levels of miR-218 in the PFC are consistent traits of mice susceptible to chronic stress and of major depressive disorder in humans. Remarkably, upregulation of *Dcc* in mouse PFC pyramidal neurons causes vulnerability to stress-induced social avoidance and anhedonia.

CONCLUSION—These data are the first demonstration of miRNA regulation of *DCC* and suggest that, by regulating *DCC*, miR-218 may be a switch of susceptibility versus resilience to stress-related disorders.

Keywords

microRNA; guidance cue; resilience; major depressive disorder; neurodevelopment; chronic social defeat stress

INTRODUCTION

The netrin-1 guidance cue receptor, DCC (deleted in colorectal cancer), directs growing axons towards appropriate targets and organizes fine neuronal connectivity across the lifespan by controlling target recognition, axon arborization, and synapse formation (1–3). Variations in *DCC* expression appear to bring about resilience or susceptibility to psychiatric disorders involving prefrontal cortex (PFC) dysfunction (4,5). *Dcc* haploinsufficiency in mice protects against the development of adult phenotypes that resemble traits observed in PFC-related psychopathologies, including deficits in cognitive flexibility and behavioral inhibition (4–6). In contrast, DCC expression in the PFC is increased in putative rodent models of these disorders (5,7). Most notably, *DCC* mRNA expression is upregulated (~50%) in the PFC of non-medicated depressed individuals who died by suicide in comparison to psychiatrically-healthy sudden death controls (4).*DCC* and its molecular regulators may be targets of protective or risk factors and serve as biomarkers of vulnerability. Currently, however, there is a lack of information about the mechanisms controlling *DCC* gene expression in the brain and about how environmental challenges modulate these processes.

MicroRNAs (miRNAS) are non-coding RNAs (~22 nucleotides) that regulate gene expression at a posttranscriptional level. By binding to the 3′-untranslated region (3′UTR) of a target mRNA, miRNAs induce RNA transcript degradation or prevent mRNA translation (8). Altered expression of miRNAs in the brain has been associated with major psychiatric conditions, including MDD (9–11). Indeed, the control that miRNAs exert on gene expression is emerging as an important molecular link between environmental risk factors and psychopathology (11–14). Here we combined postmortem human brain tissue analysis and mouse models of stress-induced psychopathologies to investigate whether *(a)*

DCC expression is under miRNA regulation and *(b)* variations in *DCC* expression in the PFC confer vulnerability to depression-like behaviors.

MATERIALS AND METHODS

Detailed description of procedures is provided in Supplemental Materials and Methods.

Animals

Experimental procedures were performed in accordance with the guidelines of the Canadian Council of Animal Care, and approved by the McGill University and Douglas Hospital Animal Care Committee.

Adult male C57BL/6 wild-type mice (PD 75±15) and male CD-1 retired breeder mice (<4 months) were obtained from Charles River, Canada. $Dcc^{lox/lox}$ mice (PD 75±15) were obtained from Dr. Berns (University of Amsterdam) (15) and are bred at the Neurophenotyping center of the Douglas Mental Health University Institute. See Supplemental Materials and Methods for further details.

Chronic social defeat stress paradigm (CSDS)

The CSDS protocol we used as in (16,17) and consisted of 10 daily sessions in which an adult wild-type C57BL/6 experimental mouse was exposed to 5min of physical aggression by a novel CD-1 mouse, previously screened for aggressive behavior. Control C57BL/6 mice were housed with a different littermate every day but no physical contact was permitted. Twenty-four hours after the last CSDS session, C57BL/6 mice were assessed in the social interaction test (17). Briefly, mice were allowed to explore an open field in the absence (session 1) or presence (session 2) of a novel CD1 mouse for a period of 2.5min each session. The social interaction ratio was calculated (time spent in the interaction zone with CD-1 present/time spent in the interaction zone with CD-1 absent) and defeated mice were classified as susceptible (ratio<1) or resilient (ratio≥1) (16). Complete description of the CSDS is available in Supplemental Materials and Methods.

Behavioral testing

Test for elevated plus maze, sucrose preference and fear conditioning were conducted as described in Supplemental Materials and Methods.

Antibodies

All the antibodies used in this study and their specificity are described in detail in Table S1 in Supplemental Materials and Methods.

Tissue dissection

Mice were euthanized by decapitation 24h after the social interaction test. Bilateral punches of the pregenual medial PFC (mPFC) were taken from 1mm coronal sections corresponding to plates 15–18 of the Paxinos & Franklin mouse atlas (18) as previously (6,7). Ventral tegmental area (VTA) punches from 1mm coronal were obtained as described previously (19). See Supplemental Materials and Methods for further details.

Western blot

mPFC tissue punches were processed for western immunoblot as before (6,19). Protein samples (25μg) were separated on a 10% SDS-PAGE and transferred to a nitrocellulose membrane which was incubated with antibodies against DCC (BD Pharmingen, Mississauga, ON, Canada) and α-tubulin (Sigma-Aldrich, Oakville, ON, Canada) (Table S1). See Supplemental Materials and Methods for details.

RNA extraction and quantitative real time-PCR for mouse tissue

Total RNA, including microRNA fraction, was isolated with the miRNeasy Micro-Kit protocol (Qiagen, Toronto, ON, Canada). Reverse transcription was performed using iScript (Bio-Rad, Saint-Laurent, QC, Canada). Real time PCR was carried out with an Applied Biosystems 7900HT RT-PCR system. Complete description of the procedure is available in Supplemental Materials and Methods.

Neuroanatomical experiments with mouse brain tissue

Mice were anesthetized with overdose injection of ketamine 50mg/kg, xylazine 5mg/kg, and acepromazine 1mg/kg (i.p) and perfused transcardially with 0.9% saline and 4% PFA in PBS. Double-labeled immunofluorescence was performed on coronal sections of the pregenual mPFC (Table S1). Immunostaining was visualized with either Alexa 488-, Alexa Fluor 555- or Alexa Fluor 633-conjugated secondary antibodies (Life technologies, Toronto, ON, Canada). See Table S1 and Supplemental Materials and Methods for details.

In situ hybridization

Frozen coronal sections of the pregenual mPFC were treated with sense and antisense 5′ digoxigenin-labeled LNA probes against miR-218 (Table S2). PFC tissue was incubated with anti-DIG antibody coupled to horseradish peroxidase (Roche, Mississauga, ON, Canada) and anti-DCC antibody #2473 (20). MiRNA expression and DCC immunofluorescence were revealed with tyramide-coupled to Cy3 (Perkin Elmer, Montréal, QC, Canada) and Alexa 488-coupled secondary antibody (Life Technologies, Toronto, ON, Canada), respectively. Complete description is available in Supplemental Materials and Methods.

In silico analysis and miRNA identification

Candidate miRNAs to regulate DCC expression were predicted using five miRNA target prediction databases: miRWalk (21), miR and a (22), miRDB (23), Diana-microT (24), and TargetScan (25). Only miRNAs that were predicted by at least three out of the five databases and were confirmed to be expressed in human and mouse brain were selected for downstream experiments. MiRNAs were ranked according to their mirSVR predicting score, which is a prediction system that determines the potential of a miRNA to regulate the expression of specific target genes (26), and selected the miRNA with the highest mirSVR score.

Quantification of miR-218 and *DCC* expression in human brain samples

The expression of miR-218 and *DCC* was quantified in prefrontal cortex (Brodmann area 44; BA44) tissue samples obtained from two different cohorts, using Real Time PCR. Complete description is available in Supplemental Materials and Methods.

Validation cohort

11 depressed subjects who committed suicide and 12 sudden-death controls. All depressed subjects were antidepressant-free for at least 3-months prior to death by suicide. A subset of this group had history of substance abuse (n=4).

Original cohort

24 depressed subjects who committed suicide and 35 sudden-death controls. The depressed group included subjects with comorbid MDD and substance abuse (n=2) to match the diagnostic characteristics of the validation cohort.

RNA isolation and quantitative Real time-PCR for human tissue

Total RNA (including miRNA fraction) was isolated from human postmortem frozen brain tissue as we reported previously (4). Total mRNA was reverse transcribed using M-MLV reverse transcriptase and oligo (dT) 16 primers. miRNA was reverse transcribed using TaqMan RT-PCR microRNA assays (Table S2; Applied Biosystems, Toronto, ON, Canada). Real-time PCR reactions were run in technical quadruplets using the ABI 7900HT Fast Real-Time PCR System (Applied Biosystems, Toronto, ON, Canada). Expression levels were calculated using the Absolute Quantitation (AQ) standard curve method, with *GAPDH* used as the reference gene for mRNA quantification and RNU6B for miRNA. The efficiencies of RT-PCR ranged between 90% and 110%, with slopes between −3.10 to −3.50. See details in Supplemental Materials and Methods.

Neuroanatomical experiment with human brain tissue

Coronal sections (14μm-thick) derived from BA44 and corresponding to plates 09 to 10 of the human brain atlas (27) were treated as described in detail in Supplemental Materials and Methods.

Human neuroblastoma IMR-32 cell line

IMR-32 cells were kindly provided by Dr. Lamarche-Vane (McGill University). IMR-32 cells were culture in Dulbecco's modified Eagle's medium (DMEM; Wisent Inc., Saint-Jean-Baptiste, QC, Canada) containing 10% fetal bovine serum, supplemented with 50 units/ml penicillin and 50μg/ml streptomycin (Invitrogen, Toronto, ON, Canada) in a 5% CO_2 humidified incubator at 37°C.

DCC immunofluorescence

Culture IMR-32 cells were platted on glass coverslips for 24h. Cells were fixed with 4% PFA and were permeabilized with 0.1% Tween in PBS and blocked with 2% BSA and 2% Goat serum. Incubation against DCC antibody #2473 (20) in blocking solution was performed overnight at 4°C, see Supplemental Materials and Methods.

Western blot

IMR-32 cells were harvested from DMEM medium and cleaned with PBS before homogenization. Protein samples (25μg) were processed for immunoblotting as described above (6).

MiRNA Mimic transfection experiment

A total of $4x10^5$ IMR-32 cells were grown in the continuous presence of either transfection reagent alone (Mock), a miR-218 mimic (5nM), or a miR-mimic scramble (5nM) control for 24h, according to the manufacturer's protocol (Qiagen, Toronto, ON, Canada). A mimic is a synthetic double-stranded miRNA that comprises the same function as endogenous miRNAs (28).

Target protector experiment

A total of $4x10^5$ cells were grown for 24hr with transfection reagent alone, or transfection reagent in combination of the miR-218 mimic and two target protectors, according to the manufacturer's protocol (Qiagen, Toronto, ON, Canada). A target protector is an oligonucleotide designed to prevent miRNAs from binding specific mRNA targets (28). Confluent cultures were homogenized using the miRNeasy Mini-Kit (Qiagen, Toronto, ON, Canada). The expression of *DCC* mRNA, *ROBO1* mRNA and miR-218 were assessed with real time PCR as described above.

Stereotaxic surgery

Adult $Dcc^{lox/lox}$ mice were deeply anesthetized with Isoflurane and placed in a stereotaxic apparatus. A total volume of 0.5μl of Adeno-Associated Virus (AAV8) expressing a Cre-GFP fusion protein under the control of the calcium calmodulin kinase II alpha (CaMKIIα) promoter (AAV8-CaMKIIα-Cre-GFP) or control virus (AAV8-CaMKIIα-GFP) was infused bilaterally into the prelimbic/infralimbic subregion of the mPFC: +2mm (A/P), ±0.5mm (M/L), and −2.7mm (D/V) relative to Bregma. Viral constructs were obtained from University of North Carolina (UNC Vector Core, Chapel Hill, NC, USA). Mice were allowed to recover for 21 days before behavioral and neuroanatomical experiments. Additional details are described in Supplemental Materials and Methods.

Stereology

The total number of SMI-32-positive pyramidal neurons at the site of injection between PrL and IL subregions of the mPFC was estimated using a stereological fractionator sampling design, with the optical fractionator probe of the Stereo Investigator® software (MicroBrightField, Williston, VT, USA) as described in detail in Supplemental Materials and Methods.

Statistical analysis

All values were represented as scatterplot with the mean ± s.e.m. A significance threshold of $\alpha<0.05$ was used in all the experiments. Statistical differences between two groups were analyzed with Student's t-tests. Correlations were calculated using the Pearson correlation

coefficient with one-tailed analysis. Otherwise one-way or two-way ANOVAs were performed, followed by Bonferroni's or Tukey's multiple comparison tests.

RESULTS

First, we tested the validity of our previous finding (4) by measuring *DCC* mRNA expression in an independent PFC sample derived from postmortem brains of 11 antidepressant-free subjects with MDD who committed suicide and of 12 psychiatrically-healthy sudden death controls (Figure 1A). Indeed, we confirmed increased *DCC* mRNA expression (~40%) in the MDD group as compared to controls (Figure 1B). Despite differences in sample size, the magnitude of *DCC* overexpression is similar between the independent studies emphasizing the consistency of this trait. From here onwards we use "validation" to refer to this second cohort and "original" to refer to the original cohort (4).

To investigate possible mechanisms underlying *DCC* upregulation in depression we explored the role of miRNAs, which fine-tune gene expression with high spatiotemporal selectivity (11). We identified miRNAs that could regulate *DCC* by cross-referencing candidates predicted by five web-based algorithms. We selected only miRNAs predicted by at least three databases and expressed in human and mouse brain. Twelve miRNAs met our criteria (Figure 1C - Table S3). We focused on miR-218 because it has the highest mirSVR score (i.e. the potential of a miRNA to regulate the expression of a target gene) (26) and is regulated in rodent PFC by chronic corticosterone treatment (29).

We performed quantitative real-time PCR (qRT-PCR) on RNA obtained from the same PFC postmortem tissue we used in our original study (4) (Figure 1D). The expression of miR-218 in the PFC is *reduced* (~50%) in the MDD versus control group (Figure 1E). Moreover, there is a negative correlation between *DCC* and miR-218 expression in the depressed group only (Figure 1F - FigureS1). To validate this finding, we measured miR-218 expression in PFC tissue derived from the validation cohort and again found reduced expression in the depressed group (Figure 1G). Therefore, increased *DCC* and reduced miR-218 expression in the PFC thus seems to be a robust finding in depression and is consistent with the inverse relationship between miRNAs and gene expression (8). Indeed, DCC and miR-218 co-express in single PFC neurons in postmortem brains from adult psychiatrically-healthy subjects, consistent with a direct miR-218-*DCC* interaction (Figure 1H–I).

As shown in Table S3, miR-1237 is a primate-specific miRNA expressed in brain that has the second highest probability to regulate *DCC* (mirSVR score= −1.22). Thus, we assessed for changes in its expression in PFC postmortem tissue obtained from the original human cohort. We found no differences in miR-1237 expression between depressed-suicide and control groups (Figure S3).

We next examined whether mice that develop depression-like phenotypes show changes in *DCC* and miR-218 expression in the mPFC similar to those observed in depressed humans. We used the chronic social defeat stress (CSDS) paradigm (30), a validated mouse model of depression that differentiates between resilient and susceptible mouse populations based on a social interaction test (16) (Figure 2A−B). Similar to humans, susceptible mice exhibit

greater PFC *Dcc* mRNA (~40%) and protein expression as compared to resilient and control mice (Figure 2C). Furthermore, PFC miR-218 expression is *diminished* in susceptible mice (~50%) in comparison to resilient and control groups (Figure 2C). Finally, as in humans, there is robust DCC and miR-218 co-expression in single PFC neurons in adult stress-naïve mice (Figure 2D).

Several reports demonstrate that CSDS induces molecular and physiologic abnormalities in VTA dopamine neurons (16,30,31). Thus, it is possible that the stress-induced changes in *Dcc* and miR-218 expression in the PFC of susceptible mice are associated with similar changes in the VTA. To this end we measured *Dcc* and miR-218 expression in the VTA of control, susceptible, and resilient mice one day after the social interaction test. However, we did not find differences in *Dcc* or miR-218 levels in the VTA between groups (Figure S4), suggesting that the *Dcc* and miR-218 alterations observed in susceptible mice are PFC-specific.

Because most, if not all, pyramidal neurons across all cortical layers are DCC-positive (Figure 3A), we next micro infused AAV-CaMKIIα-CreGFP or AAV-CaMKIIα-GFP (control vector) bilaterally into the PFC of adult $Dcc^{lox/lox}$ mice to delete *Dcc* from pyramidal neurons exclusively. Mice were exposed toCSDS3 weeks later (Figure 3B). Socially-defeated $Dcc^{lox/lox}$ mice infected with control vector display the expected social avoidance; an effect lost in mice infected with the Cre-expressing vector (Figure 3C). Defeated $Dcc^{lox/lox}$ mice infected with control vector also spend more time in the corners farthest away from the interaction zone when the social target is present than control mice that did not undergo CSDS. This behavior is completely prevented in defeated mice that had *Dcc* deletion in PFC pyramidal neurons (Figure 3D). Importantly, results from fear conditioning experiments indicate that *Dcc* deletion from PFC pyramidal neurons does not lead to learning deficits (Figure S5). Furthermore, locomotor activity is not altered by *Dcc* deletion (Figure 3E).

We also tested sucrose preference in $Dcc^{lox/lox}$ mice that received control or AAV-CaMKIIα-CreGFP infections and underwent CSDS or served as controls. Defeated $Dcc^{lox/lox}$ mice infected with control vector show less sucrose preference than control mice that did not undergo CSDS. *Dcc* deletion from PFC pyramidal neurons prevents this anhedonia-like effect (Figure 3F). Finally, we exposed mice to the elevated plus maze and found that CSDS-exposed mice, regardless of viral infection, display a pro-anxiety-like effect (Figure 3G). Thus, knocking out *Dcc* from pyramidal neurons in PFC results in resilience against stress-induced depression-like phenotypes specifically.

Brain sections through the medial PFC of mice injected with AAV-CaMKIIα-CreGFP or AAV-CaMKIIα-GFP viruses were triple immunolabeled with GFP (green), DCC (red), and SMI-32 (blue; neurofilament heavy antibody; which is a marker for pyramidal neurons (32)). A robust decrease in DCC immunoreactivity was observed in SMI-32-positive pyramidal neurons infected with the AAV-CaMKIIα-CreGFP virus, but not with the control AAV-CaMKIIα-GFP (Figure 3H). This is in line with our previous *Dcc* knock-out experiments using $Dcc^{lox/lox}$ mice and similar viral-mediated gene transfer techniques (4). Importantly, the expression of the AAV-CaMKIIα-GFP control construct or with AAV-CaMKIIα-

CreGFP (along with the accompanying loss of DCC expression) does not compromise SMI-32 neuron survival (Figure 3I) and it is specific to pyramidal neurons (Figure S6).

To investigate the regulation of *DCC* expression by miR-218, we used the human neuroblastoma cell line IMR-32 which expresses endogenous *DCC* mRNA and protein (Figure 4A). IMR-32 cells transfected with a synthetic miR-218 ("mimic") *decreases DCC* expression 24h after treatment (Figure 4B). We confirmed *overexpression* of miR-218 in IMR-32 cells that received the mimic (Figure 4C). The 3′UTR of *DCC* contains two binding sites for miR-218, from nucleotides 66–73 (binding site 1) and from 513–518 (binding site 2; Figure 4D). To prove that miR-218 binds directly to *DCC* and downregulates its expression, we transfected IMR-32 cells with single-stranded and modified RNAs ("target protectors") designed to interfere with the two binding sites between miR-218 and the 3′UTR of *DCC* without affecting other targets (Figure 4E). Remarkably, these target protectors *reverse* completely the downregulation in *DCC* expression induced by the miR-218 mimic (Figure 4F).

To further test the specificity of the *DCC*-selective target protector, we measured the mRNA levels of *ROBO1*; the receptor of the guidance cue, Slit, and a validated target of miR-218 (33–35). Transfection with the miR-218 mimic alone indeed results in a significant downregulation in the expression of *ROBO1* mRNA (~45%). Importantly, cells treated with the *DCC*-selective target protector also show miR-218 mimic-induced downregulation of *ROBO1* mRNA (Figure 4G). This result demonstrates specificity of the target protector for *DCC* and miR-218 binding. To our knowledge this is the first demonstration thatmiR-218 binds directly to *DCC* mRNA to repress its expression and that this mechanism occurs in nerve cells.

DISCUSSION

An understanding of the pathophysiology of stress-related disorders, including MDD, is necessary for developing novel preventive strategies and overcoming the lack of effectiveness of current treatments. One way to advance this knowledge is to identify candidate molecular determinants of vulnerability and of resiliency using post-mortem human brain tissue of subjects who manifest such conditions. Another strategy is to take advantage of pre-clinical models to characterize the enduring plastic alterations occurring in the brain caused by stress. In this study we combined these two approaches and demonstrated that increased *DCC* expression in PFC neurons causes susceptibility to stress-induced depressive-like behaviors whereas dampened *DCC* expression is protective. These findings are in line with our idea that DCC receptors mediate detrimental, enduring effects of environmental risk factors, but are also involved in conferring resilience (4,5,36). Therefore, the expression of *DCC* and/or of its molecular regulators could serve as a biomarker of vulnerability to MDD.

In this study we identified miR-218 as a repressor of *DCC* gene expression and found a significant *reduction* in miR-218 expression in the PFC of (a) adult mice that are susceptible to chronic stress-induced social avoidance and (b) adult non-medicated human with MDD who died by suicide. In fact, the expression of miR-218 and *DCC* in the PFC are negatively

correlated in MDD. These findings indicate that miR-218 could potentially serve as both a non-invasive biomarker of *DCC* function and a target of therapeutic interventions. MicroRNAs can be measured in blood with the advantage of being stable and resistant to changes in temperature (37). Furthermore, levels of circulating miRNAs can change in parallel to alterations in brain expression (38) and have been shown after antidepressant treatment (9) and cognitive behavioral therapy (10) and are promising predictors of antidepressant response (9).

Whether increased *Dcc* expression in susceptible mice to chronic stress is a preexisting factor or results from exposure to chronic social defeat stress is an important question to be elucidated in future experiments. DCC protein expression in the mouse PFC is high during embryonic and early postnatal age, but decreases substantially in adolescence, achieving low levels in adulthood (39). It is possible that susceptible mice fail to show downregulation of DCC expression in adolescence and that its enduring elevated levels in the PFC alter the structural and functional maturation of PFC pyramidal neurons, rendering this region more vulnerable to detrimental effects of chronic stress. We are currently examining changes in circulating miR-218 as a result of adverse experiences in adult mice and whether these alterations match those induced in the PFC.

Our previous work on the development of the dopamine system shows that DCC signaling within VTA dopamine neurons determines the extent of their innervation to the PFC (4,40). Importantly, this effect is restricted to the adolescent period and can be modified by exposure to drugs of abuse during this age (41). Furthermore, by controlling dopamine input to the PFC in adolescence, DCC determines the structural maturation of PFC pyramidal neurons (4). The fact that adult exposure to CSDS does not lead to changes in *Dcc* and miR-218 in the VTA suggests that the changes observed in PFC of susceptible mice are not initiated by altered *Dcc* function within dopamine neurons. Future experiments will determine whether chronic stress in adolescence (e.g. social isolation) regulates DCC and miR-218 in both PFC and VTA and whether these changes are causally related. It is intriguing that CSDS in adulthood induces a decrease in the firing activity of mesocortical dopamine neurons and that selective inhibition of these neurons leads to social avoidance in mice (31). It would be interesting to establish whether inhibition of the mesocortical dopamine pathway leads to reduce miR-218 in the adult PFC and, in turn, to increase *Dcc* expression.

To assess the role of *Dcc* in stress-induced social avoidance and anhedonia we used a homozygous knockout of *Dcc* in pyramidal neurons. However, in our previous studies we have shown that variations, rather than absence, of DCC protein result in alterations in neuronal connectivity and plasticity (4). Moreover, complete knockout of *Dcc* may lead to compensatory changes that could diminish the effects of *Dcc* on normal neuronal function. In the future we plan to assess whether knocking down *Dcc* in single PFC pyramidal neurons also confers resilience to stress-induced social avoidance and anhedonia and whether *Dcc* haploinsufficient mice show resistance against or reduced sensitivity to chronic social defeat stress. Notably, *DCC* haploinsufficiency exists in humans (42,43).

How variations in *DCC* expression lead to susceptibility or resilience to depression-like behaviors remains to be determined. During development, DCC receptors guide growing axons towards Netrin-1-secreting targets (44). However, DCC receptors also dictate the fine organization of synaptic connectivity by controlling axon arborization, dendritic growth (45) and synapse formation (46). These different actions are specific to particular brain systems and maturational states, including adulthood, and are modified by experience (5). By tuning *DCC* expression in PFC pyramidal neurons, miR-218 may lead to subtle, but very distinct changes in pyramidal neuron synaptic connectivity. Interestingly, miR-218 has been shown to repress the expression of the guidance cue receptors, Roundabout (Robo)-1 and 2(47). Robo-1 and DCC can form receptor complexes to alter axonal responses to Netrin-1(48). MiR-218 may thus act as a spatiotemporal regulator of guidance cue receptor genes to orchestrate the effects of environmental risk and protective factors across the lifespan.

Supplementary Material

Refer to Web version on PubMed Central for supplementary material.

Acknowledgments

This work was funded by Canadian Institute for Health Research (C.F. MOP-74709), the National Institute on Drug Abuse (C. F. Grant number: R01DA037911), the Natural Science and Engineering Research Council of Canada (C.F. Grant Number 2982226), and National Institute of Mental Health (E.J.N. Grant number: P50MH096890). C.F. is a research scholar of the Fonds de Recherche du Québec - Santé. J.P.L. received a Frederick Banting and Charles Best Canada Graduate Scholarships doctoral funding award from CIHR.

References

1. Moore SW, Tessier-Lavigne M, Kennedy TE. Netrins and Their receptors. Adv Exp Med Biol. 2007; 621:17–31. [PubMed: 18269208]
2. Shen K, Cowan CW. Guidance Molecules in Synapse Formation and Plasticity. Cold Spring Harb Perspect Biol. 2010; 2:a001842. [PubMed: 20452946]
3. Finci L, Zhang Y, Meijers R, Wang JH. Signaling mechanism of the netrin-1 receptor DCC in axon guidance. Prog Biophys Mol Biol. 2015; 118:153–160. [PubMed: 25881791]
4. Manitt C, Eng C, Pokinko M, Ryan RT, Torres-Berrio A, Lopez JP, Yogendran SV, et al. dcc orchestrates the development of the prefrontal cortex during adolescence and is altered in psychiatric patients. Transl Psychiatry. 2013; 3:e338. [PubMed: 24346136]
5. Flores C. Role of netrin-1 in the organization and function of the mesocorticolimbic dopamine system. J Psychiatry Neurosci. 2011; 36:296–310. [PubMed: 21481303]
6. Grant A, Hoops D, Labelle-Dumais C, Prévost M, Rajabi H, Kolb B, Stewart J, et al. Netrin-1 receptor-deficient mice show enhanced mesocortical dopamine transmission and blunted behavioural responses to amphetamine. Eur J Neurosci. 2007; 26:3215–3228. [PubMed: 18005074]
7. Flores C, Bhardwaj SK, Labelle-Dumais C, Srivastava LK. Altered netrin-1 receptor expression in dopamine terminal regions following neonatal ventral hippocampal lesions in the rat. Synapse. 2009; 63:54–60. [PubMed: 18932228]
8. Bartel DP. MicroRNAs: genomics, biogenesis, mechanism, and function. Cell. 2004; 116:281–297. [PubMed: 14744438]
9. Lopez JP, Lim R, Cruceanu C, Crapper L, Fasano C, Labonte B, Maussion G, et al. miR-1202 is a primate-specific and brain-enriched microRNA involved in major depression and antidepressant treatment. Nat Med. 2014; 20:764–768. [PubMed: 24908571]
10. Issler O, Haramati S, Paul, Evan D, Maeno H, Navon I, Zwang R, Gil S, et al. MicroRNA 135 Is Essential for Chronic Stress Resiliency, Antidepressant Efficacy, and Intact Serotonergic Activity. Neuron. 2014; 83:344–360. [PubMed: 24952960]

11. O'Connor RM, Dinan TG, Cryan JF. Little things on which happiness depends: microRNAs as novel therapeutic targets for the treatment of anxiety and depression. Mol Psychiatry. 2012; 17:359–376. [PubMed: 22182940]
12. Kolshus E, Dalton VS, Ryan KM, McLoughlin DM. When less is more – microRNAs and psychiatric disorders. Acta Psychiatr Scand. 2014; 129:241–256. [PubMed: 23952691]
13. Caputo V, Ciolfi A, Macri S, Pizzuti A. The Emerging Role of MicroRNA in Schizophrenia. CNS Neurol Disord Drug Targets. 2015; 14:208–221. [PubMed: 25613509]
14. Kenny PJ. Epigenetics, microRNA, and addiction. Dialogues Clin Neurosci. 2014; 16:335–344. [PubMed: 25364284]
15. Krimpenfort P, Song J-Y, Proost N, Zevenhoven J, Jonkers J, Berns A. Deleted in colorectal carcinoma suppresses metastasis in p53-deficient mammary tumours. Nature. 2012; 482:538–541. [PubMed: 22358843]
16. Krishnan V, Han M-H, Graham DL, Berton O, Renthal W, Russo SJ, LaPlant Q, et al. Molecular Adaptations Underlying Susceptibility and Resistance to Social Defeat in Brain Reward Regions. Cell. 2007; 131:391–404. [PubMed: 17956738]
17. Golden SA, Covington HE, Berton O, Russo SJ. A standardized protocol for repeated social defeat stress in mice. Nat Protocols. 2011; 6:1183–1191. [PubMed: 21799487]
18. Paxinos, G.; Franklin, K. Paxinos and Franklin's the Mouse Brain in Stereotaxic Coordinates. Boston, Amsterdam: Elsevier/Academic Press; 2013.
19. Manitt C, Labelle-Dumais C, Eng C, Grant A, Mimee A, Stroh T, Flores C. Peri-Pubertal Emergence of UNC-5 Homologue Expression by Dopamine Neurons in Rodents. PLoS ONE. 2010; 5:e11463. [PubMed: 20628609]
20. Seaman C, Anderson R, Emery B, Cooper HM. Localization of the netrin guidance receptor, DCC, in the developing peripheral and enteric nervous systems. Mech Dev. 2001; 103:173–175. [PubMed: 11335129]
21. Dweep H, Sticht C, Pandey P, Gretz N. miRWalk – Database: Prediction of possible miRNA binding sites by "walking" the genes of three genomes. J Biomed Inform. 2011; 44:839–847. [PubMed: 21605702]
22. Betel D, Wilson M, Gabow A, Marks DS, Sander C. The microRNA.org resource: targets and expression. Nucl Acids Res. 2008; 36:D149–D153. [PubMed: 18158296]
23. Wang X. miRDB: A microRNA target prediction and functional annotation database with a wiki interface. RNA. 2008; 14:1012–1017. [PubMed: 18426918]
24. Maragkakis M, Reczko M, Simossis VA, Alexiou P, Papadopoulos GL, Dalamagas T, Giannopoulos G, et al. DIANA-microT web server: elucidating microRNA functions through target prediction. Nucl Acids Res. 2009; 37:W273–W276. [PubMed: 19406924]
25. Lewis BP, Shih Ih, Jones-Rhoades MW, Bartel DP, Burge CB. Prediction of Mammalian MicroRNA Targets. Cell. 2003; 115:787–798. [PubMed: 14697198]
26. Betel D, Koppal A, Agius P, Sander C, Leslie C. Comprehensive modeling of microRNA targets predicts functional non-conserved and non-canonical sites. Genome Biol. 2010; 11:R90. [PubMed: 20799968]
27. Mai, J.; Paxinos, G.; Voss, T. Atlas of the Human Brain. San Diego: Elsevier/Academic Press; 2007.
28. Small EM, Olson EN. Pervasive roles of microRNAs in cardiovascular biology. Nature. 2011; 469:336–342. [PubMed: 21248840]
29. Dwivedi Y, Roy B, Lugli G, Rizavi H, Zhang H, Smalheiser NR. Chronic corticosterone-mediated dysregulation of microRNA network in prefrontal cortex of rats: relevance to depression pathophysiology. Transl Psychiatry. 2015; 5:e682. [PubMed: 26575223]
30. Berton O, McClung CA, DiLeone RJ, Krishnan V, Renthal W, Russo SJ, Graham D, et al. Essential Role of BDNF in the Mesolimbic Dopamine Pathway in Social Defeat Stress. Science. 2006; 311:864–868. [PubMed: 16469931]
31. Chaudhury D, Walsh JJ, Friedman AK, Juarez B, Ku SM, Koo JW, Ferguson D, et al. Rapid regulation of depression-related behaviours by control of midbrain dopamine neurons. Nature. 2013; 493:532–536. [PubMed: 23235832]

32. Campbell MJ, Morrison JH. Monoclonal antibody to neurofilament protein (SMI-32) labels a subpopulation of pyramidal neurons in the human and monkey neocortex. J Comp Neurol. 1989; 282:191–205. [PubMed: 2496154]
33. Fish JE, Wythe JD, Xiao T, Bruneau BG, Stainier DYR, Srivastava D, Woo S. A Slit/miR-218/Robo regulatory loop is required during heart tube formation in zebrafish. Development. 2011; 138:1409–1419. [PubMed: 21385766]
34. Amin ND, Bai G, Klug JR, Bonanomi D, Pankratz MT, Gifford WD, Hinckley CA, et al. Loss of motoneuron-specific microRNA-218 causes systemic neuromuscular failure. Science. 2015; 350:1525–1529. [PubMed: 26680198]
35. Thiebes KP, Nam H, Cambronne XA, Shen R, Glasgow SM, Cho H-H, Kwon J-s, et al. miR-218 is essential to establish motor neuron fate as a downstream effector of Isl1-Lhx3. Nat Commun. 2015:6.
36. Dunn EC, Wiste A, Radmanesh F, Almli LM, Gogarten SM, Sofer T, Faul JD, et al. Genome-Wide Association Study (GWAS) and Genome-Wide by Environment Interaction Study (GWEIS) of Depressive Symptoms in African American and Hispanic/Latina Women. Depress Anxiety. 2016; 33:265–280. [PubMed: 27038408]
37. Chakraborty C, Das S. Profiling cell-free and circulating miRNA: a clinical diagnostic tool for different cancers. Tumour Biol. 2016:1–10.
38. Rao P, Benito E, Fischer A. MicroRNAs as biomarkers for CNS disease. Front Mol Neurosci. 2013; 6:1–13.
39. Goldman JS, Ashour MA, Magdesian MH, Tritsch NX, Harris SN, Christofi N, Chemali R, et al. Netrin-1 Promotes Excitatory Synaptogenesis between Cortical Neurons by Initiating Synapse Assembly. J Neurosci. 2013; 33:17278–17289. [PubMed: 24174661]
40. Manitt C, Mimee A, Eng C, Pokinko M, Stroh T, Cooper HM, Kolb B, et al. The Netrin Receptor DCC Is Required in the Pubertal Organization of Mesocortical Dopamine Circuitry. J Neurosci. 2011; 31:8381–8394. [PubMed: 21653843]
41. Reynolds LM, Makowski CS, Yogendran SV, Kiessling S, Cermakian N, Flores C. Amphetamine in Adolescence Disrupts the Development of Medial Prefrontal Cortex Dopamine Connectivity in a dcc-Dependent Manner. Neuropsychopharmacology. 2015; 40:1101–1112. [PubMed: 25336209]
42. Srour M, Rivière J-B, Pham JMT, Dubé M-P, Girard S, Morin S, Dion PA, et al. Mutations in DCC Cause Congenital Mirror Movements. Science. 2010; 328:592–592. [PubMed: 20431009]
43. Depienne C, Cincotta M, Billot S, Bouteiller D, Groppa S, Brochard V, Flamand C, et al. A novel DCC mutation and genetic heterogeneity in congenital mirror movements. Neurology. 2011; 76:260–264. [PubMed: 21242494]
44. Manitt C, Kennedy TE. Chapter 32 Where the rubber meets the road: netrin expression and function in developing and adult nervous systems. Prog Brain Res. 2002; 137:425–442. [PubMed: 12440385]
45. Teichmann HM, Shen K. UNC-6 and UNC-40 promote dendritic growth through PAR-4 in Caenorhabditis elegans neurons. Nat Neurosci. 2011; 14:165–172. [PubMed: 21186357]
46. Colón-Ramos DA, Margeta MA, Shen K. Glia Promote Local Synaptogenesis Through UNC-6 (Netrin) Signaling in C. elegans. Science. 2007; 318:103–106. [PubMed: 17916735]
47. Small EM, Sutherland LB, Rajagopalan KN, Wang S, Olson EN. MicroRNA-218 Regulates Vascular Patterning by Modulation of Slit-Robo Signaling. Circ Res. 2010; 107:1336–1344. [PubMed: 20947829]
48. Stein E, Tessier-Lavigne M. Hierarchical Organization of Guidance Receptors: Silencing of Netrin Attraction by Slit Through a Robo/DCC Receptor Complex. Science. 2001; 291:1928–1938. [PubMed: 11239147]

A

Validation cohort

	Control	MDD
Sample	12	11
Sex	12 M	11 M
Age	36.6 ± 3.2	38.5 ± 3.5
RIN	6.6 ± 0.2	6.4 ± 0.3
PMI	30.6 ± 5.3	41.6 ± 5.4
Brain pH	6.5 ± 0.08	6.4 ± 0.08

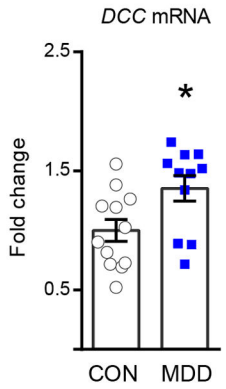

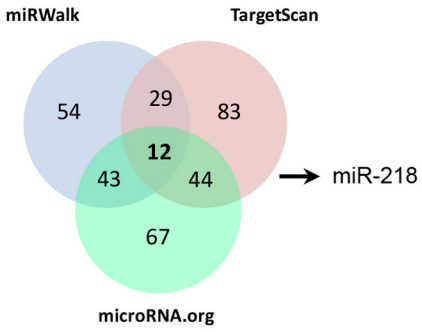

D

Original cohort

	Control	MDD
Sample	35	24
Sex	31 M / 4 F	22 M / 2 F
Age	47.5 ± 3.6	43.8 ± 3.3
RIN	6.6 ± 0.12	6.8 ± 0.2
PMI	42.9 ± 4.6	40.8 ± 3.5
Brain pH	6.5 ± 0.05	6.6 ± 0.07

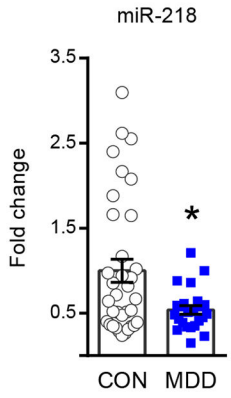

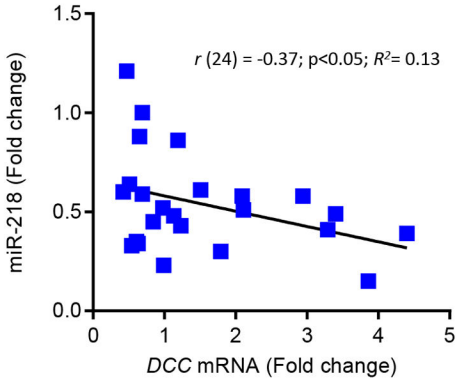

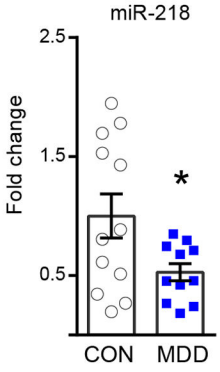

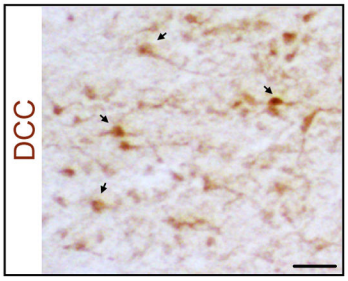

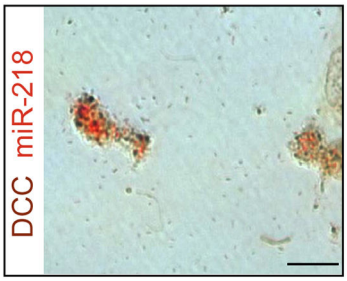

Figure 1.

Opposite *DCC* and miR-218 regulation in PFC in MDD. **(A)** Summary of the information about the age and gender of the human subjects in the validation cohort. Brain samples were compared for age, RNA integrity number (RIN), post-mortem intervals (PMI), and pH value. There are no differences between groups (Age: $t_{(21)}$=0.39; RIN: $t_{(21)}$=0.55; PMI: $t_{(21)}$= 1.44; pH: $t_{(21)}$=0.92, *p* values >0.05). **(B)** *DCC* mRNA in the PFC is increased in MDD versus controls ($t_{(21)}$=2.50;**p*=0.02) in the validation cohort. **(C)** miRNAs predicted to bind *DCC*. **(D)** Summary of the information about subjects in the original cohort. There are no

differences between groups (Age: $t_{(57)}$=0.71; RIN: $t_{(57)}$=t=0.84; PMI: $t_{(57)}$= 0.33; pH: $t_{(57)}$=1.25). **(E)** Reduction in miR-218 in depressed versus control groups ($t_{(57)}$=2.71;*p=0.008) in original cohort (4). **(F)** Negative *DCC*-miR-218 correlation in MDD. **(G)** Decreased miR-218 in PFC of depressed versus control groups in validation cohort ($t_{(21)}$=2.30;*p=0.031). **(H)** DCC+ neurons and **(I)** DCC and miR-218 co-expression in PFC neurons. Scale bar= 50μm. The error bars represent the SEM.

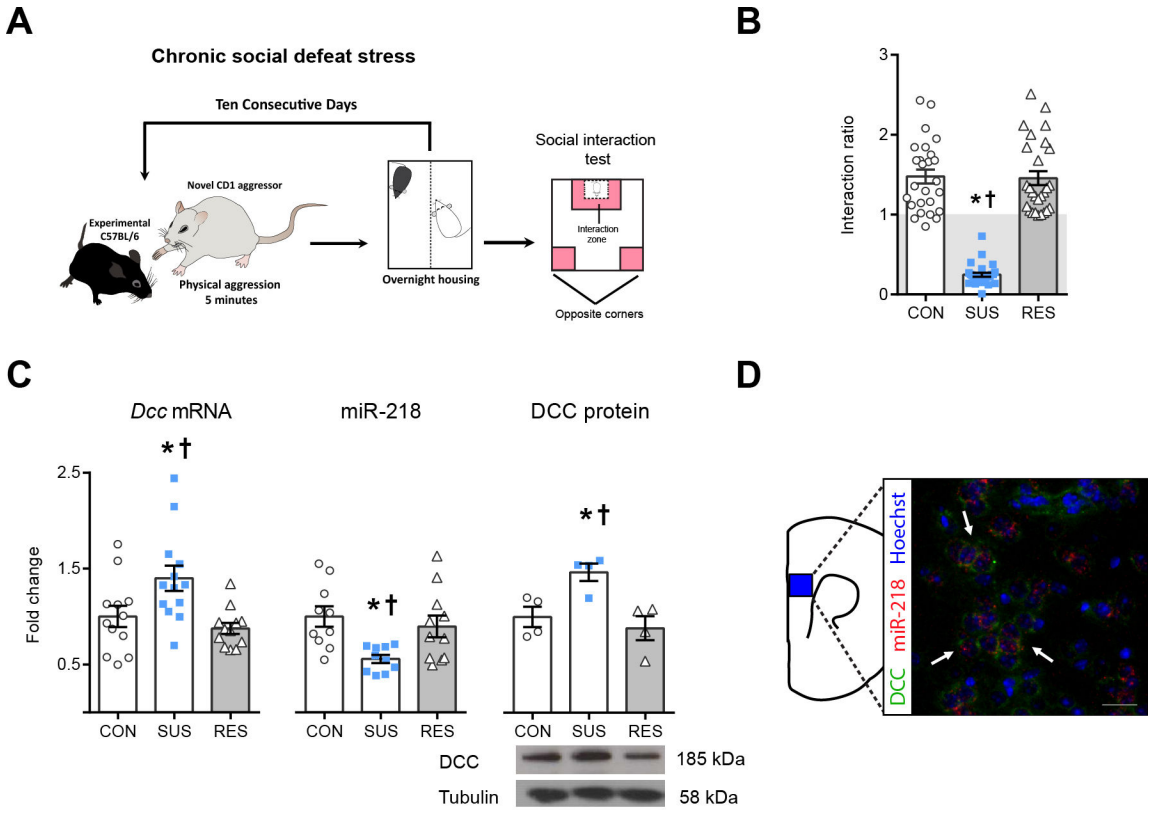

Figure 2.

Opposite expression of *Dcc* and miR-218 in PFC is associated with susceptibility to stress-induced depression-like behaviors. *† indicate different from control (CON) and resilient (RES), respectively. **(A)** CSDS protocol. **(B)** Social interaction ratio in CON (n=26), susceptible (SUS; n=27) and RES (n=27). $F_{(2,77)}$=94.37;p< 0.0001;*†p<0.01. **(C)** Increased PFC *Dcc* expression in SUS (n=12–13; $F_{(2,34)}$=6.725;p=0.003,*†p<0.01). Decreased PFC miR-218 expression in SUS (n=10–11; $F_{(2,28)}$=5.85; p=0.0075,*p<0.01; †p<0.05). Elevated PFC DCC protein in SUS (n= 4; $F_{(2,9)}$= 8.085; p=0.098, *†p<0.05). The mRNA, microRNA, and protein data were derived from tissue samples of susceptible, resilient and control mice collected from 3 different and independent CSDS experiments.**(D)** Co-expression of DCC/miR-218 in PFC neurons. Scale bars =50 μm.

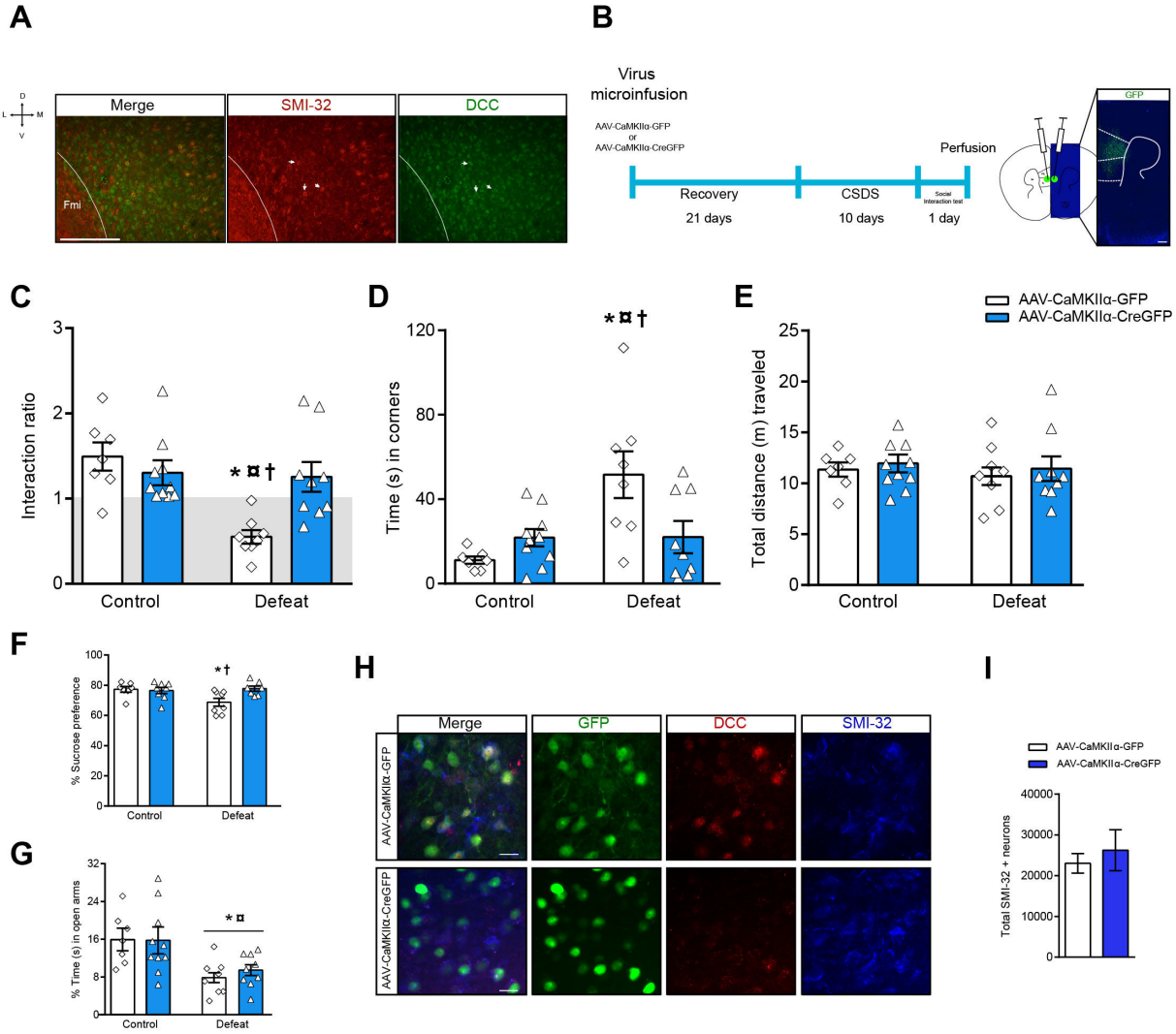

Figure 3.

Knocking out *Dcc* in PFC pyramidal neurons protects against stress-induced depression-like behaviors. **(A)** DCC expression in SMI-32+ medial PFC pyramidal neurons in adult stress-naïve mice (white arrows). **(B)** Timeline of infection experiments and injection site. PFC pyramidal neuron *Dcc* deletion prevents social avoidance induced by CSDS. **(C)** Ratio: Two-way ANOVA: stress: $F_{(1,30)}$=10.91; p=0.0025; stress by virus interaction: $F_{(1,30)}$=8.87; p=0.0057; Tuckey test: *¤†p<0.05. **(D)** Corners: Two-way ANOVA: stress: $F_{(1,30)}$=8.77; p=0.0059; stress by virus interaction: $F_{(1,30)}$=7.83; p=0.0089;*†p<0.05, ¤p<0.01. Symbols indicate different from *control-AAV-CaMKIIα-GFP (n=7), ¤control-AAV-CaMKIIα-Cre-GFP (n=10) and †defeat-AAV-CaMKIIα-Cre-GFP (n=9); p<0.05.**(E)** Locomotor activity during the social interaction test is similar across all groups: Two-way ANOVA: stress by virus interaction: $F_{(1,30)}$= 0.004; p= 0.94, group: $F_{(1,30)}$= 0.36; p= 0.55, and virus: $F_{(1,30)}$=0.48; p=0.49).**(F)** Sucrose preference: Two-way ANOVA: stress by virus interaction: $F_{(1,26)}$=5.26; p=0.030. **(G)** Deletion of *Dcc* does not prevent anxiety-related behaviors induced by CSDS: Two-way ANOVA: significant main effect of stress, $F_{(1,30)}$=15.81; p=0.0004; *different from control; p<0.05). **(H)** Deletion of *Dcc* in individual GFP+/

SMI-32+ neurons **(I)** Stereological analysis show that *Dcc* deletion does not compromise the survival of medial PFC SMI-32+ neurons ($t_{(8)}$= 0.57, p=0.58). Scale bars =50 μm.

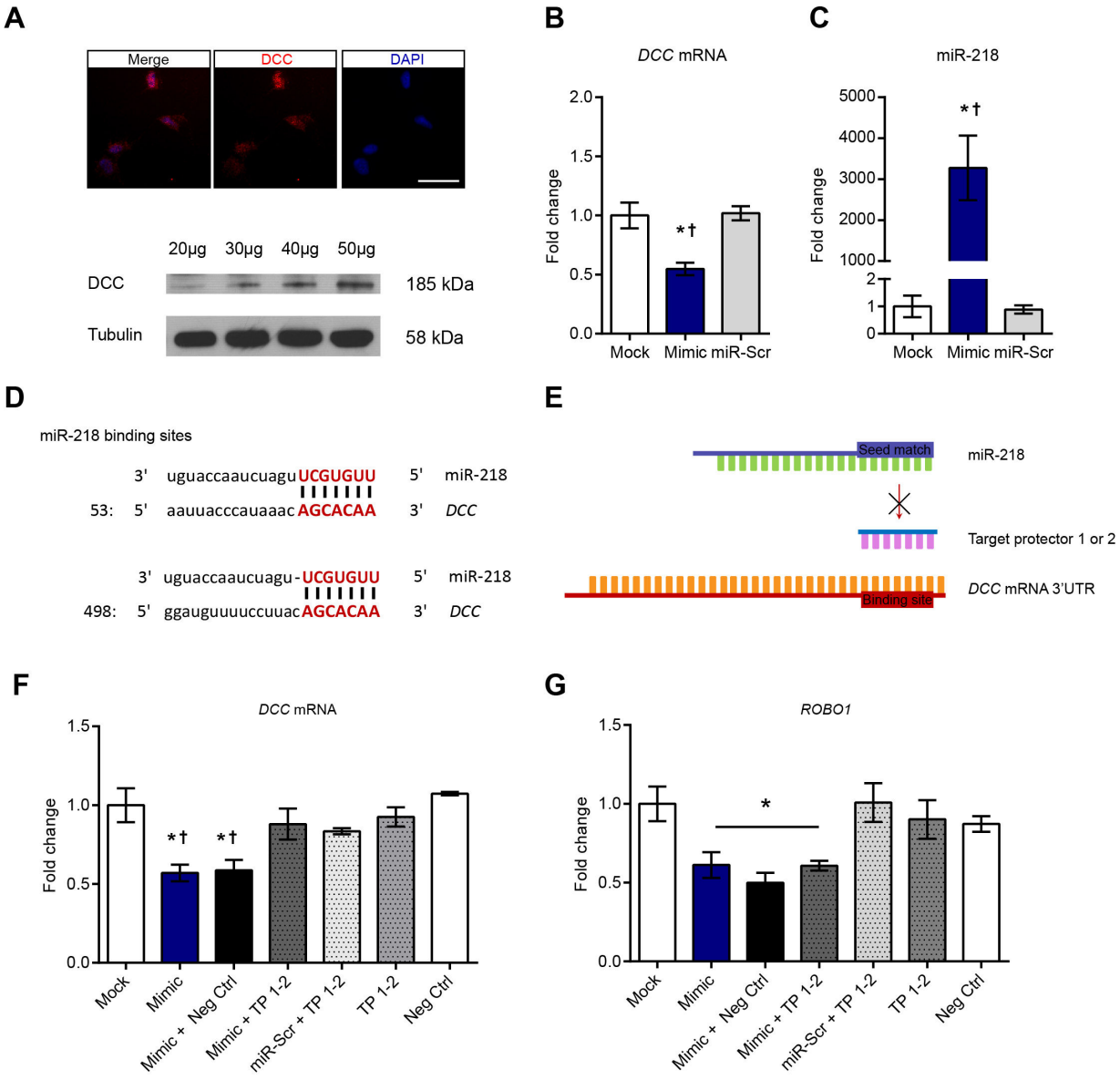

Figure 4.

miR-218 regulates *DCC* expression.**(A)** Immunofluorescence and Western blot experiments showing endogenous DCC expression in the IMR-32 cell line. Numbers on top of the DCC bands represent micrograms of protein loaded. Scale bar= 50µm. **(B)** Significant decreased of *DCC* mRNA expression in IMR-32 cells 24h after transfection with a miR-218 mimic (n=3) in comparison to transfection with reagent alone (mock; n=3) or mimic scramble (miR-Scr; n=3) ($F_{(2,6)}$=11.75; p=0.008; *different from mock; †different from miR-Scr, *†p<0.05). **(C)** Transfection with mimic in comparison to transfection reagent (mock) or mimic scrambled (miR-Scr) increases miR-218 in IMR-32 cells 24h after. One-way ANOVA: $F_{(2,6)}$=17.25; p<0.01; *different from mock; †different from miR-Scr; *†p<0.001). **(D)** miR-218 and *DCC* base pairing at the two binding sites. **(E)** Target protector experiment. **(F)** Decreased *DCC* expression in IMR-32 cells by miR-218 mimic 24 after transfection is reversed by target protectors ($F_{(6,16)}$=5.493; p= 0.0030; *different from mock;

†different from negative control *p<0.05). n=3–5. **(G)** miR-218-induced downregulation of *ROBO1* in IMR-32 cells is not prevented by *DCC*-specific target protectors ($F_{(6,16)}$= 4.546; p= 0.0071; *different from mock. *p<0.05). n=3–5.